frontiers | Frontiers in Materials

ORIGINAL RESEARCH
published: 17 May 2022
doi: 10.3389/fmats.2022.914994

Conductive GelMA/PEDOT: PSS Hybrid Hydrogel as a Neural Stem Cell Niche for Treating Cerebral Ischemia-Reperfusion Injury

Yilei Zhang[1,2,3†], Meimei Zhang[1,2†], Runlin Zhang[4†], Haining Liu[1,2], Hui Chen[1,2], Xiaofeng Zhang[1,2], Chen Li[1,2,5], Qing Zeng[1,2], Yunhua Chen[4*] and Guozhi Huang[1,2*]*

[1]Department of Rehabilitation Medicine, Zhujiang Hospital, Southern Medical University, Guangzhou, China, [2]School of Rehabilitation Medicine, Southern Medical University, Guangzhou, China, [3]Department of Neurorehabilitation Medicine, Xiangya Boai Rehabilitation Hospital, Changsha, China, [4]School of Materials Science and Engineering, South China University of Technology, Guangzhou, China, [5]Department of Rehabilitation Medicine, Hunan Provincial People's Hospital, Hunan Normal University, Changsha, China

OPEN ACCESS

Edited by:
Mingqiang Li,
Third Affiliated Hospital of Sun Yat-sen University, China

Reviewed by:
Gao Liang,
Guangdong University of Technology, China
Wei Wang,
Tianjin University, China
Huanan Wang,
Dalian University of Technology, China

***Correspondence:**
Qing Zeng
zengqingyang203@126.com
Yunhua Chen
msyhchen@scut.edu.cn
Guozhi Huang
drhuang66@163.com

†These authors have contributed equally to this work

Specialty section:
This article was submitted to Biomaterials, a section of the journal Frontiers in Materials

Received: 07 April 2022
Accepted: 21 April 2022
Published: 17 May 2022

Citation:
Zhang Y, Zhang M, Zhang R, Liu H, Chen H, Zhang X, Li C, Zeng Q, Chen Y and Huang G (2022) Conductive GelMA/PEDOT: PSS Hybrid Hydrogel as a Neural Stem Cell Niche for Treating Cerebral Ischemia-Reperfusion Injury. Front. Mater. 9:914994. doi: 10.3389/fmats.2022.914994

Cerebral ischemia and the subsequent cerebral ischemia-reperfusion (I/R) injury usually result in neuronal impairment with serious disabilities. Although neural stem cell (NSC) transplantation can help with functional recovery after stroke, due to the improper cellular milieu after brain injury, direct NSC transplantation will result low cell survival rates and differentiation efficiency into neurons. Here a conductive hybrid hydrogel based on gelatin methacryloyl (GelMA) and poly(3,4-ethylenedioxythiophene): poly (styrene sulfonate) (PEDOT:PSS) was created as a NSC niche for the treatment of cerebral I/R injury. GelMA/PEDOT:PSS hybrid hydrogel promoted the development of NSCs into neurons. GelMA/PEDOT:PSS hydrogel along with NSCs could enhance neuronal activity and minimize apoptosis when co-cultured with oxygen-glucose deprivation/reperfusion (OGD/R) neurons. Furthermore, after 7 days of implantation, GelMA/PEDOT:PSS/NSCs on the infarcted brain of rats subjected to reperfusion injury after middle cerebral artery occlusion (MCAO) was verified to attenuate inflammatory responses. These findings show that the conductive GelMA/PEDOT:PSS hybrid hydrogel could regulate NSC development and act as promising cell niches for the treatment of cerebral I/R injury.

Keywords: conductive hybrid hydrogel, neural stem cells, 3D culture, cell differentiation, cerebral ischemiareperfusion injury

1 INTRODUCTION

Stroke, cerebral ischemia infarction in particular, is rapidly becoming the main global cause of long-term disability and mortality globally (Naghavi et al., 2017; Tuo et al., 2022). Despite its high prevalence, patients with ischemic stroke have limited therapy options. During the acute stroke period, tissue plasminogen activator and rapid recanalization (thrombectomy) are still being used. However, due to the short therapeutic window and significant risk of intracerebral hemorrhage, individuals who have suffered a stroke cannot just rely on these therapies (Fann et al., 2013; Stonesifer et al., 2017). It is generally believed that the ideal treatment for cerebral infarction should involve replacing the damaged neurons and promoting the proliferation and differentiation of neural stem cells (NSCs), thus improving the patient outcomes (Felling and Song 2015).

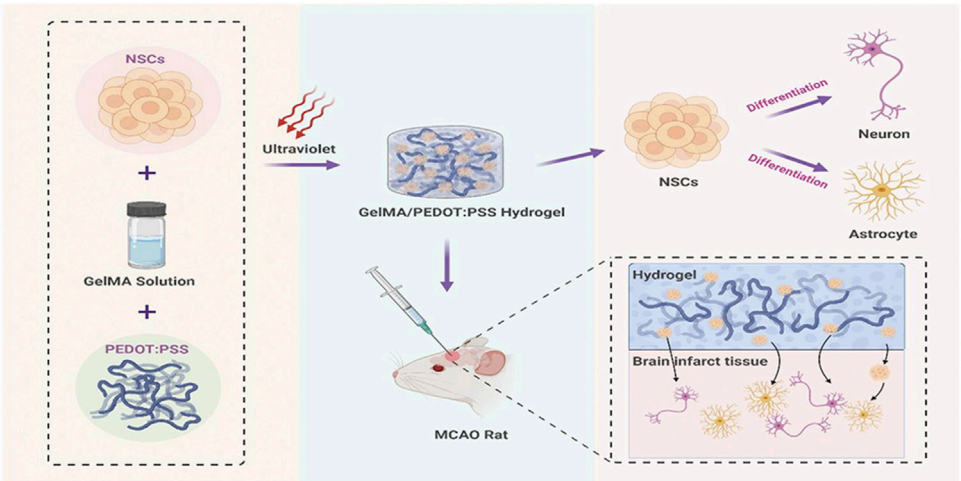

FIGURE 1 | Scheme. Conductive GelMA/PEDOT:PSS hybrid hydrogel to promote NSCs differentiation and treat cerebral I/R injury.

NSC therapy has emerged as a cutting-edge therapeutic technique in recent years. Cell differentiation, cell replacement, immune regulation, neural network repair, and nutritional factor release are mechanisms by which NSC transplantation enhances stroke prognosis (Zhou et al., 2021). NSCs delivery in the early stroke phase attenuates this complex inflammatory signaling cascade (Bacigaluppi et al., 2009; De Feo et al., 2012). NSCs ameliorate ischemic damage by lowering pro-inflammatory mediators including TNF-α, IL-1β, IL-6, MCP-1, and iba-1(Huang and Zhang 2019). However, NSC transplantation has not yet produced the expected therapeutic results (Burns and Quinones-Hinojosa 2021). One possible reason for its low effectiveness of this method can be the limited survival of transplanted NSCs in the damaged cerebral areas. The transplanted cells do not get integrated into the host system and differentiate quickly into neurons (Tang et al., 2015). This could primarily occur owing to an unfavorable environment for transplanted NSCs in the infarcted brain after a stroke (Ju et al., 2014).

Interestingly, various biomaterial scaffolds have been used to support stem cell therapy. Hydrogels were used to help with tissue repair and regeneration in the central nervous system (CNS) (Woerly 1993). For example, the potential of gelatin methacryloyl (GelMA) in facilitating cell adhesion and proliferation, for example, has been established, and it is now considered a suitable biological material for three dimensional (3D) varied cell cultures (Wang et al., 2017; Ning et al., 2020). Conducting polymers, on the other hand, have been used in neural recovery because endogenous bioelectric signals are critical for maintaining neuronal function, neurite growth, and secretion of neurotrophic factors (Lee et al., 2009; Levin et al., 2017). However, the biological application of conductive polymers has been limited due to drawbacks such as low processability, hydrophobicity, and poor degradability. The most common method for overcoming these drawbacks is to combine the benefits of both materials (Balint et al., 2014). Dissolvable inert particles (Yang and Martin 2004) and biodegradable polymer fibers, for example, can be used as a template for conducting polymers (Abidian et al., 2006). Because of its better electrical conductivity and chemical stability, poly(3,4-ethylenedioxythiophene)-poly(styrenesulfonate) (PEDOT: PSS), a derivative of polythiophene, is one of the most promising conductive polymers. PEDOT: PSS in a soft hydrogel matrix has been proven to improve dorsal root ganglion differentiation (Fitria 2019). It would be appealing to combine GelMA and PEDOT: PSS to generate a conductive hydrogel to be used as a NSCs niche to promote its differentiation. However, to the best of our knowledge, there is no such study in this regard. Moreover, the neuroprotective effect of hydrogel in combination with NSCs on oxygen-glucose depribation/reperfusion (OGD/R) neurons as well as on cerebral I/R injury remain unidentified.

In this study, a conductive GelMA/PEDOT: PSS hybrid hydrogel has been developed under photo-initiated polymerization and more importantly utilized as NSCs niche to stimulate neuron development and treat cerebral I/R injury (**Figure 1**). The *in vitro* results demonstrated that the hybrid hydrogel with good biocompatibility might stimulate differentiation in NSCs into neurons. When co-cultured with OGD/R neurons, NSCs embedded in the GelMA/PEDOT:PSS hydrogel showed neuroprotective benefits. Furthermore, following 7 days of implantation, the GelMA/PEDOT:PSS/NSCs significantly reduced inflammatory responses in a rat model of middle cerebral artery occlusion (MCAO), even showed the function of protecting damaged neurons, suggesting that the conductive GelMA/PEDOT:PSS hydrogel could serve as a promising NSC niche for the treatment of cerebral I/R injury.

2 MATERIALS AND METHODS

2.1 Hydrogel Preparation and Characterization

2.1.1 Materials

GelMA was purchased from Yongqin-Quan Intelligent Equipment Co., Ltd. (Suzhou, China). PEDOT:PSS was

provided by Sigma-Aldrich. Lithium Phenyl(2,4,6-trimethylbenzoyl)phosphinate (LAP) has already embed in the GelMA hydrogel by Yongqin-Quan Intelligent Equipment Co., Ltd. Other reagents are of analytical grade and are used as received.

2.1.2 Gelatin Methacryloyl/ Poly(3,4-Ethylenedioxythiophene): Poly (Styrene Sulfonate) Hydrogel Preparation

PEDOT:PSS was ultrasonically dissolved in PBS at varying concentrations (0%, 0.005%, 0.01%, and 0.015% w/v). The mixture (1 ml) was then agitated at 40°C with 60 mg of GelMA. Finally, the GelMA/PEDOT:PSS hydrogels were set for 18 s under Ultraviolet light (UV) light (405 nm). GelMA, GelMA/PEDOT:PSS50, GelMA/PEDOT:PSS100, and GelMA/PEDOT:PSS150 represented hydrogels with PEDOT:PSS concentrations of 0%, 0.005%, 0.01%, and 0.015% w/v.

2.1.3 Gelatin Methacryloyl/ Poly(3,4-Ethylenedioxythiophene): Poly (Styrene Sulfonate) Hydrogel Morphology

Scanning electron microscopy (SEM, FEI Q25) was used to investigate the macroporous structure of lyophilized GelMA/PEDOT: PSS hydrogels. The fracture surface of hydrogels was detected under SEM after gold sputtering.

2.1.4 Compressive Mechanical Properties

Compressive stress-strain of the hydrogels was tested using a dynamic mechanical analyzer (DMA Q800, United States). Compression and compressive cycle tests were performed on cylindrical hydrogel samples (8-mm diameter and 10-mm thickness). Compression testing was conducted in a strain control mode at a linear rate of 50% per minute from 0% to 100%, whereas compression cycle testing was repeated 10 times at a strain rate of 100% per minute in the strain range of 0%–30%.

2.1.5 Conductivity Measurement

A Fluke F17B+ digital multimeter was used to study the electrical conductivity of GelMA/PEDOT: PSS hydrogels (Guangzhou Ruice Electronic Technology Co., Ltd.). The conductivity was computed using the following formula: $\sigma = l/R \times S$, where l is the hydrogels' height, R is the hydrogels' resistance, and S is the hydrogels' contacting area. The hydrogel resistance was determined by calculating the average of three measurements.

2.2 Cell Viability and Proliferation Analysis

As previously stated, NSCs were extracted from the embryonic brains of Sprague-Dawley rats (gestation days 13–15; provided by the Experimental Animal Center of South Medical University in China) (Zhou et al., 2020). NSCs encased in a variety of PEDOT: On day 3, 5, and 7, PSS concentrations of GelMA solution were employed in a CCK-8 assay to determine proliferation. Briefly, a hydrogel precursor comprising 6% GelMA was dissolved in PBS and combined with PEDOT: PSS in varying concentrations (0%, 0.005%, 0.01%, and 0.015% w/v). The absorbance OD value at 450 nm was measured using a microplate reader. Cells planted in GelMA hydrogels were used as conrtols. The viability of NSCs was determined using LIVE/DEAD dyes (Apexbio, Suzhou, China) in accordance with the manufacturer's instructions, and a Leica THUNDER Imager DM18 was used to capture images under a microscope.

2.3 *In Vitro* Immunocytochemistry

Immunocytochemical analysis was performed to examine the differentiation of NSCs encapsulated within the 3D GelMA/PEDOT:PSS hydrogels, as previously described (Wang et al., 2018). Briefly, NSCs (1×10^5) were co-cultured in 24-well plates each well using various GelMA/PEDOT:PSS hydrogels. On day 7, the NSCs in the hydrogels were fixed for 15 min at room temperature with 4% formaldehyde. The cells were incubated in PBS containing 0.1% TritonX-100 for 5 min at room temperature and permeabilized with 10% serum for 1 h at room temperature. The samples were then incubated overnight with MAP2 and GFAP as primary antibodies at 4°C. After three gentle washes with PBS, secondary antibodies were incubated with the sample for 2 h at room temperature in the dark. The cells were finally stained with DAPI after three gentle washes with PBS.

2.4 Gene Expression Analysis

As previously stated, the expression levels of NSCs cultured for 7 days in different hydrogel concentrations were examined using quantitative reverse transcription-polymerase chain reaction (qRT-PCR) (Lu et al., 2018). To release the contained NSCs, the hydrogels were first decomposed in a 0.3 mg/ml GelMA pyrolysis liquid solution (Yongqin-Quan Intelligent Equipment Co., Ltd., China). RNAiso Plus was then used to extract the total RNA from the NSCs (TaKaRa, Japan). A PrimeScript RT reagent Kit with a gDNA Eraser was used to conduct the cDNA reverse transcription reaction (Accurate Biotechnology Co., Ltd.). The SYBR Green Premix Pro Taq HS qPCR Kit was used to perform qPCR (Accurate Biotechnology Co., Ltd.). The primers were manufactured by Sangon Biotech (Shanghai, China), and the NSC primer sequences for β tubulin-III, MAP2, and GFAP are listed in **Table 1**. As an internal control, glyceraldehyde 3-phosphate dehydrogenase (GAPDH) was used.

2.5 Co-Culturing Oxygen-Glucose Deprivation/Reperfusion Neurons and Gelatin Methacryloyl/ Poly(3,4-Ethylenedioxythiophene): Poly (Styrene Sulfonate)/Neural Stem Cell

Based on previous research, primary neurons were extracted from 16 to 18-days old embryonic mouse brains cortex (Lin et al., 2020) and seeded on poly-L-lysine (Sigma–Aldrich)-coated plates (1.0×10^5 cells/mL). To simulate ischemia, the neurons were placed in a glucose-free Dulbecco's modified Eagle medium with 5% CO_2 and 1% O_2 for 2 h at 37°C after 7 days of normal culture (OGD). After OGD, the glucose-free medium was replaced with neurobasal media, and the mice were reintroduced to a normoxic incubator for 24 h to simulate reperfusion. The cells in the control group were cultured in a neurobasal medium and were not exposed to OGD/R (Spencer et al., 2018). To separate the neurons and hydrogel NSCs composites, transwell plates

TABLE 1 | The primer sequences for quantitative reverse transcription-polymerase chain reaction.

Rat Target Genes	Forward primers (5′–3′)	Reverse primers (5′–3′)
MAP2	AACATCCTCCGAGTCACCCTTCC	ATCTAGCATCTCAGGCAGGTCAGG
β-tubulin 3	CATGAAGGAGGTGATGACAGATG	GTTGCCGATGAAGGTGGACGAC
GFAP	CAGACCTCACAGACGTTGCTTCC	AGTTGGCGGCGATAGTCATTAGC
GAPDH	GGCACAGTCAAGGCTGAGAATG	ATGGTGGTGAAGACGCCAGTA

(Corning, United States) were used for co-culture. Primary cultured neurons were grown in the lower compartment. Following OGD/R or control treatment, NSCs (1×10^5 cells/ml), NSCs with GelMA, or NSCs with GelMA/PEDOT:PSS100 were co-cultured with neurons in the upper chamber. The neurons were harvested after 7 days of co-culture.

2.6 Hoechst 33342/Propidium Iodide Double Staining

The procedure of staining with Hoechst 33342 and propidium iodide (PI) was previously reported (Wang et al., 2018). Hoechst 33342 (Apexbio, Houston, TX, United States) was used to treat neurons, followed by PI (Apexbio, Houston, TX, United States) staining at 37°C for 15 min. Images were taken using an inverted fluorescent microscope (NIKON ECLIPSE Ti2-E), and the proportion of PI-positive cells was determined.

2.7 Histocompatibility of the Gelatin Methacryloyl/ Poly(3,4-Ethylenedioxythiophene): Poly (Styrene Sulfonate) Hybrid Hydrogel

An intraperitoneal dose of 1% pentobarbital sodium (30 mg/kg) was used to anesthetize normal Sprague-Dawley rats. The rats were shaved using a shaving knife after inducing anesthesia. The cerebral stereo positioning injection equipment was used to fix the sedated rats, and the ear rod was softly pushed into the external auditory canal. The top jaw was then fixed by inserting the upper front teeth of rats into the groove of the upper tooth fastening plate and tightening the screws. By measuring the placement needle, the anterior and posterior fontanelles are adjusted on the same sagittal line, and the anterior fontanelle (Bregma) and posterior fontanelle (Lambda) is maintained as horizontal as possible. To avoid infection, the head is disinfected with 75% alcohol. To corrode the meninges, cut 1.5 cm of the skin between the ears were cut using scissors and use 3% hydrogen peroxide was used. 20 μl of PBS, GelMA, GelMA/PEDOT:PSS100 (n = 4) subjecting to UV irradiation for 18 s, were then injected using microsyringes at the rate of 1 μl/min, respectively. A syringe with a 26 G needle was used to inject 10 μl into two distinct locations in the brain: AP + 2.3 mm, ML-3.0 mm, DV-2.3 mm and AP 0 mm, ML-3.0 mm, DV-2.3 mm (Tuladhar et al., 2020). The microsyringe was removed 5 min after the injection. After the rats were awakened, the skin incisions were cleansed using iodine and sutured; the animals were then returned to the feeding chamber. The biocompatibility of the conductive hydrogel injected into the brain was evaluated by hematoxylin and eosin (HE) staining of the brain tissue at 3 and 14 days following the injection. The samples were embedded in paraffin after paraformaldehyde cardiac perfusion fixing and dehydration. As per a previous study, the samples were sliced into 4-μm-thin cross-sections for HE staining (Ying et al., 2020).

2.8 Establishment of Middle Cerebral Artery Occlusion Model in Rats

The Southern Medical University Zhujiang Hospital Ethics Committee approved all procedures involving animals in this investigation. In a rat model of MCAO, male Sprague-Dawley rats (starting weight 250–280 g, Southern Medical University animal facility) were used, as previously described (Zhao et al., 2013). The neck hair was shaved after anesthesia, and the limbs were secured to the surgical table. Disinfect the neck skin and use scissors to make a 2 cm incision. To expose the common carotid artery and the bifurcation of the common carotid artery, the tissue surrounding the incision was torn bluntly. A suture thread was placed in a dead knot at the proximal end of the common carotid artery and a loose knot was used at the distal end of the common carotid artery to fix the threaded plug. Spring scissors were used to make an incision at the proximal end of the heart, tweezers were used to insert the threaded plug from the incision, and the external carotid artery was gently constricted using tweezers to protect the line plug. The thread plug was stopped when the black mark on the threaded plug reached the bifurcation of the common carotid artery. Indwelled sutures were used to secure the threaded plug. The body temperature was maintained by using the thermal insulation pads, and the suture plug was removed 90 min later and the surgical incision was sutured. Inclusion criteria for the MCAO model are as follows: After the rats were awake, the Longa score (She et al., 2019) was evaluated, and those with a score of 1–3 were chosen for the rest of the experiment.

2.9 Immunohistochemical Staining

After successfully establishing the MCAO rat model for 5 days, the rats were intraperitoneally with anesthetized using pentobarbital (30 mg/kg) and then mounted on a stereotaxic frame and injected with hydrogel (Liu et al., 2014). The rats were then injected with NSCs (5.0×10^6 cells/ml), NSCs mixed with GelMA/PEDOT:PSS100 hydrogels, or GelMA hydrogels, whereas the MCAO rats were treated with PBS (n = 4). The hydrogels and NSCs were fixed, mounted, flash-frozen, and sectioned after 7 days of implanting (Basara et al., 2021). Immunofluorescence labeling was performed on brain cryosections (10 μm thick) (Li et al., 2019). The primary antibodies were GFAP and iba1 (both from Abcam, Boston, MA, United States). The secondary antibodies were incubated

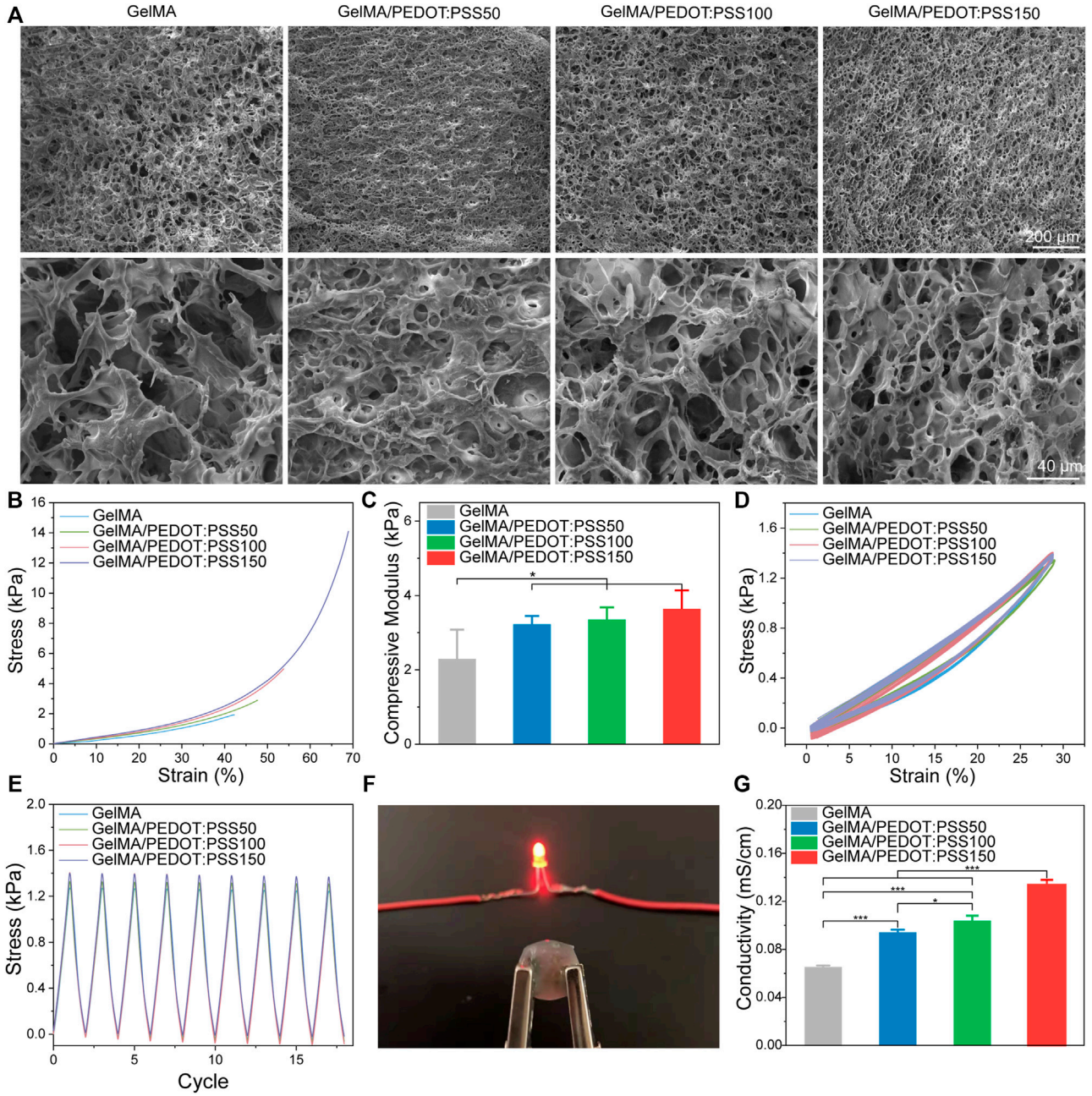

FIGURE 2 | Structural characterization and physical properties of GelMA/PEDOT: PSS hydrogels. **(A)** Internal porous morphology of GelMA/PEDOT:PSS hydrogels. **(B)** Representative compressive stress-strain curves. **(C)** Compressive moduli of GelMA/PEDOT: PSS hydrogels. **(D)** Loading-unloading curves of GelMA/PEDOT: PSS hydrogels at a strain of 30%. **(E)** Compressive stress was recovered to the initial state after repeated compression. **(F)** An LED bulb and GelMA/PEDOT: PSS100 hydrogel formed a closed circuit. **(G)** The conductivity of GelMA/PEDOT: PSS hydrogels. The data are expressed as mean ± standard deviation. $^{*}p < 0.05$, $^{**}p < 0.01$, $^{***}p < 0.001$.

with the sections for 2 h in the dark at room temperature before being gently washed three times. The nuclei were dyed for 10 min with DAPI (Solarbio, China) and then gently rinsed three times. A fluorescence microscope was used to image the slices (NIKON ECLIPSE Ti2-E). The number of regions with positive cells was counted using the ImageJ software.

2.10 Statistical Analyses

For statistical analysis, Graph Pad Prism software (version 8.0, CA) was used. All quantitative data were expressed as mean and ± standard deviation (SD). The findings were analyzed using one-way ANOVA, followed by Tukey's HSD post hoc test (for multiple groups).

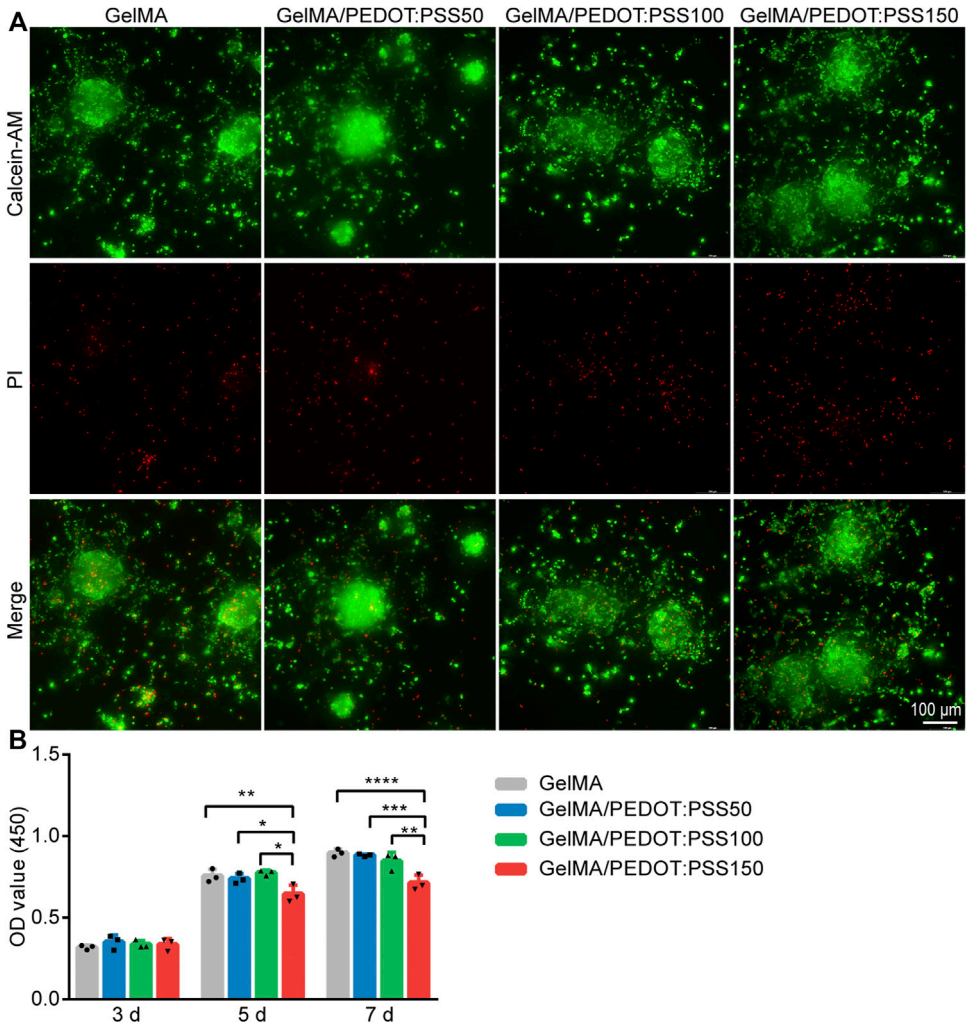

FIGURE 3 | NSC viability in the conductive GelMA/PEDOT: PSS hybrid hydrogels. **(A)** LIVE (green)/DEAD (red) NSC staining using Calcein-AM/PI staining after 7 days of culture. **(B)** Assessment of cell proliferation by the CCK-8 assay (n = 3), $^{*}p < 0.05$ $^{**}p < 0.01$ $^{***}p < 0.001$, and $^{****}p < 0.0001$.

3 RESULTS

3.1 Characterization of Conductive Gelatin Methacryloyl/ Poly(3,4-Ethylenedioxythiophene): Poly (Styrene Sulfonate) Hydrogels

GelMA/PEDOT:PSS hybrid hydrogels were facilely prepared by photo-initiation polymerization. **Figure 2A** presents the SEM images of the porous structure of GelMA/PEDOT:PSS hydrogels. The incorporation of PEDOT:PSS into the hydrogel matrices did not significantly affect the macroporous morphology of the lyophilized hydrogels. **Figure 2B** reveals how PEDOT: PSS increased the compressive stress and maximum strain of GelMA/PEDOT:PSS hydrogels. GelMA/PEDOT:PSS150 hydrogels showed a compressive stress of 14.1 kPa and a maximum strain of 68.9%, whereas GelMA hydrogels without PEDOT: PSS had compressive stress of 1.92 kPa and a maximum strain of 42.2%. **Figure 2C** shows that the compressive modulus of PSS150 and GelMA hydrogels was 3.64 and 2.30 kPa, respectively. Furthermore, the mechanical recovery of GelMA/ PEDOT: PSS hydrogels was studied during compressive cycle testing. After 10 compressive cycles, all hydrogels in **Figures 2D,E** immediately recovered to their initial stress levels. PEDOT:PSS showed considerably improved compressive strength and mechanical reversibility under cyclic compression, according to these findings. An LED bulb and GelMA/PEDOT:PSS100 hydrogel formed a closed circuit in **Figure 2F**. As demonstrated in **Figure 2G**, increasing the concentration of PEDOT:PSS enhanced the conductivity of the GelMA/PEDOT: PSS hydrogel. The conductivity of GelMA/PEDOT:PSS150 hydrogels increased substantially compared with GelMA hydrogels (0.065 ± 0.001 mS/cm) and even reached 0.134 ± 0.004 mS/cm.

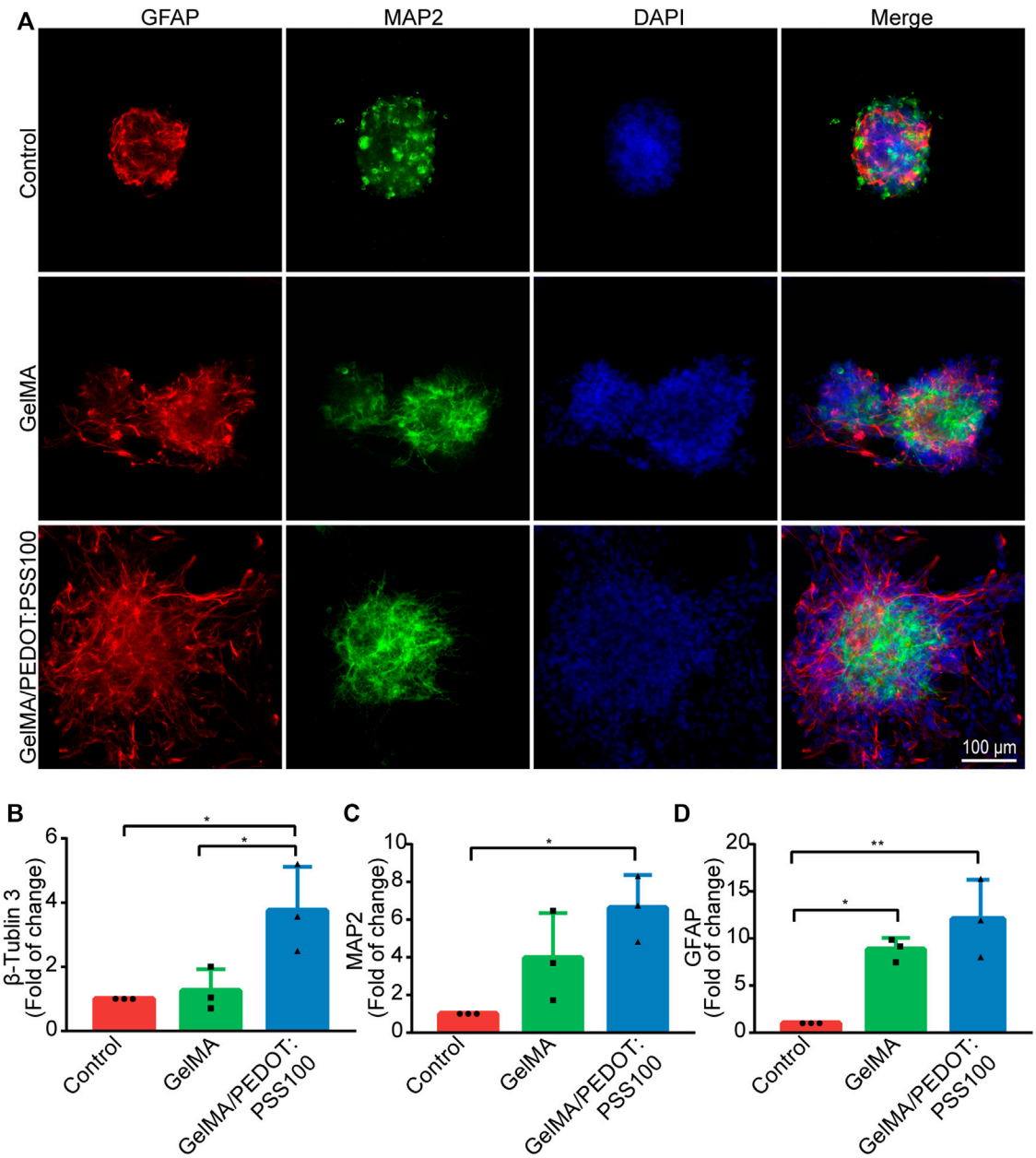

FIGURE 4 | *In vitro* immunostaining of NSCs and gene expression level of NSCs. **(A)** NSCs immunostaining images. **(B)** β-Tubulin 3, **(C)** MAP2, and **(D)** GFAP gene expression levels (n = 3). The data are expressed as mean ± standard deviation. $^{*}p < 0.05$ and $^{**}p < 0.01$.

3.2 Neural Stem Cell Viability in Conductive Gelatin Methacryloyl/ Poly(3,4-Ethylenedioxythiophene): Poly (Styrene Sulfonate) Hydrogels

Immunofluorescence staining was used to identify NSCs and their ability to differentiate into various nerve cells (**Supplementary Figure S1**). The LIVE/DEAD staining was used to determine the cytotoxicity of conductive hydrogels on day 7 (**Figure 3A**), and a CCK-8 assay was used to determine viability on day 3, 5, and 7 (**Figure 3B**). According to our findings, 6% of GelMA hydrogel-encapsulated NSCs still had spherical shapes, which is consistent with the findings of other studies (C. Li et al., 2021). The LIVE/DEAD assay revealed that the density of dead cells steadily increased as PEDOT:PSS concentrations increased.This pattern matched that of the CCK-8 assay, which showed a high level of cell viability, indicating that the GelMA hydrogel inclusion of PEDOT:PSS50/100/150 had no significant effect on cell viability on day 3 compared with the control samples without PEDOT:PSS. On day 5 and 7, however, in addition to NSC proliferation, the addition of PEDOT:PSS150

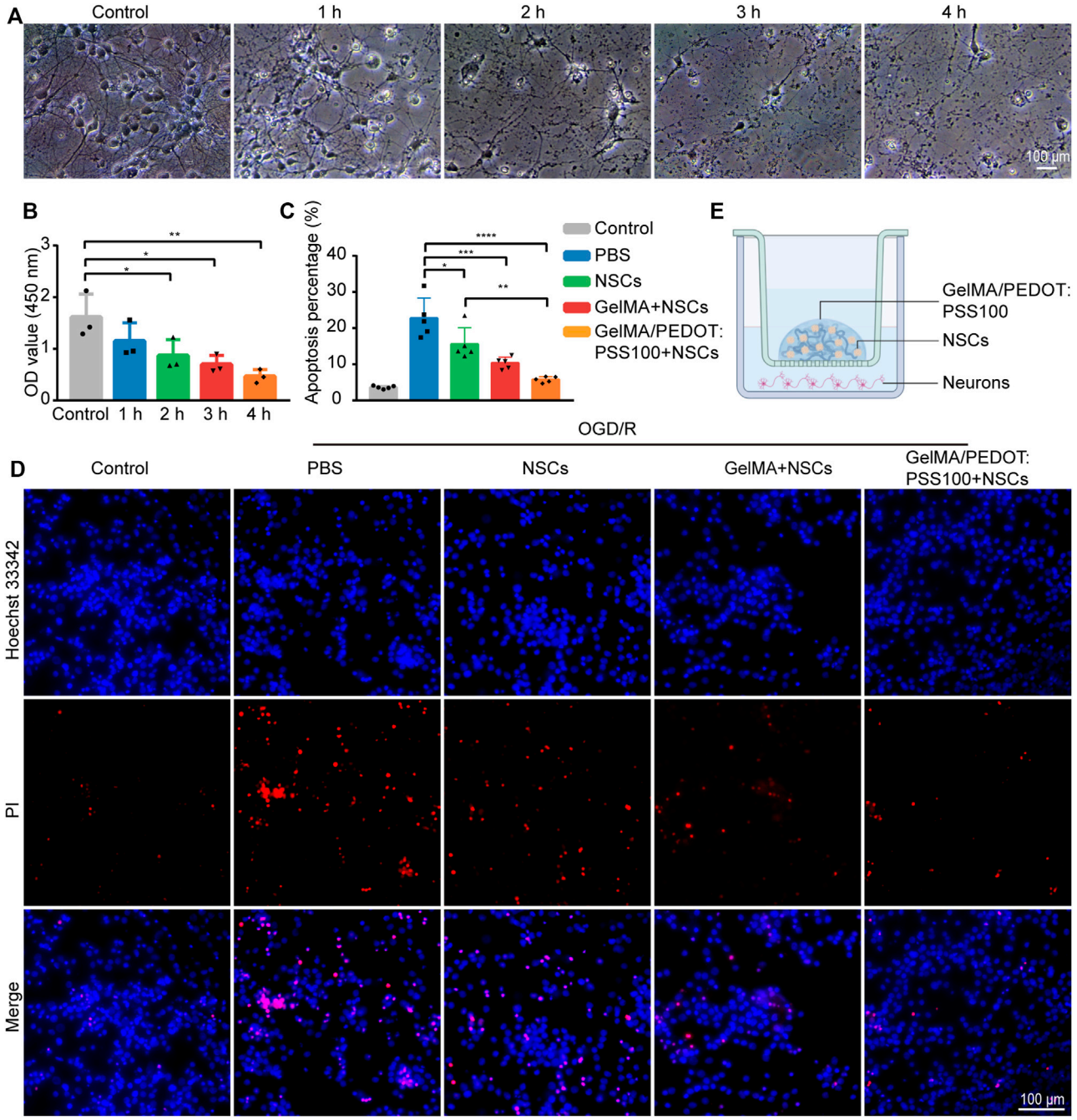

FIGURE 5 | Repairing effects on OGD/R-injured neurons. **(A)** Neuronal morphology of OGD/R-injured neurons after 1–4 h. **(B)** The cell viability was determined by the CCK-8 assay of OGD/R-injured neurons. **(C)** Analysis of the percentage of the apoptotic cells in the different OGD/R treatment groups. **(D)** Fluorescent microscopic analysis of apoptotic cells stained with PI and Hoechst 33342 in the different OGD/R treatment groups. **(E)** Diagram of Transwell co-culture system. The data are expressed as mean ± standard deviation. $^{*}p < 0.05$, $^{**}p < 0.01^{***}$, $p < 0.001$, and $^{****}p < 0.0001$.

resulted in reduced cell viability compared with other groups. We choose the optimum PEDOT:PSS concentration to form a conductive hydrogel for our next experiment based on hydrogel conductivity and NSC viability on PEDOT:PSS. GelMA/PEDOT:PSS100 may have conductive qualities as well as the best biocompatibility for NSCs. Compared with GelMA hydrogels, NSC differentiation in this conductive hydrogel was observed for 7 days.

3.3 Neural Stem Cell Differentiation in Conductive Gelatin Methacryloyl/ Poly(3,4-Ethylenedioxythiophene): Poly (Styrene Sulfonate) Hydrogels

NSCs cultured in conductive PEDOT:PSS hydrogels displayed elongated neurite outgrowth, resulting in a thin neural network, as described by Wang et al. (2018). NSCs were stained with antibodies against astrocytes and neuronal markers of GFAP and MAP2 after 7 days of culturing to observe the differentiation. The pluripotency of the NSCs was preserved, allowing them to develop into a variety of neural cell types (**Figure 4A**). The expression levels of differentiation-related genes expression in NSCs were then assessed using qRT-PCR. β Tubulin-III (**Figure 4B**), MAP2 (**Figure 4C**), and GFAP (**Figure 4D**) expression levels were found to be higher in NSCs cultured in the GelMA/PEDOT:PSS100 scaffold than in the control group. Our results showed that the GelMA/PEDOT:PSS hydrogel co-cultured with NSCs facilitated the differentiation of NSCs into astrocytes and neurons, which is comparable to the results of previously reported conductive materials for promoting NSCs differentiation (Wang et al., 2018). This also means there will be lower differentiation rate into other types of neurocytes such as oligodendrocytes.

3.4 Gelatin Methacryloyl/ Poly(3,4-Ethylenedioxythiophene): Poly (Styrene Sulfonate)/Neural Stem Cell Repairing Effect on Oxygen-Glucose Deprivation/Reperfusion-Injured Neurons

Figure 5A shows the neuronal morphology of OGD/R-injured neurons after 1–4 h. **Figure 5B** presents the CCK-8 assay results of OGD/R-injured neurons, which was used to evaluate cell viability. The OD value of neurons in the OGD/R 2 h group was half that of the control group, according to the CCK8 assay results. As a result, we chose the 2 h group for the following experiment, as described in earlier studies (Liu et al., 2014). In **Figure 5E**, we used the Transwell assay to observe the alterations in OGD/R neurons following a 7-days hydrogel intervention. The protective effects of NSCs and NSCs in hydrogels of varying concentrations were evaluated using Hoechst 33342/PI staining on damaged neurons exposed to OGD/R. Compared with the NSCs group, the percentage of apoptotic cells in the GelMA/PEDOT: PSS100/NSCs group markedly decreased dramatically (**Figures 5C,D**). These findings suggested that NSCs cultured in GelMA/PEDOT:PSS100 hydrogels could increase neuroprotective effects more effectively than NSCs alone.

3.5 Conductive Hydrogel Histocompatibility *In Vivo*

The histocompatibility of the hydrogels was determined by transcranial injection of HE staining into the brains of healthy Sprague-Dawley rats before *in vivo* application. PBS injection, GelMA injection, and GelMA/PEDOT:PSS100 injection groups (n = 4) were used in the experiments. Three days after the injection was administered, both groups showed similar amount of inflammation in their cerebral tissue. On day 14, the number of inflammatory cells had gradually decreased, and only a few inflammatory cells remained (**Figures 6A,B**). It can be seen from the HE staining results that the hydrogel group did not cause severe inflammation and tissue necrosis in the surrounding tissue compared with the sterile PBS group, indicating that the hydrogel has no toxicity to brain tissue. It was also found that the injection of PBS caused a mild inflammatory response, which could attribute to the mechanical damage caused by the syringe. However, lesions were formed after cerebral ischemia, and the tissue damage caused by the syringe was negligible. This observation is in line with the earlier report (Yuan et al., 2021). Therefore, the GelMA and GelMA/PEDOT:PSS100 hydrogels all had great biocompatibility and did not cause cerebral inflammation *in vivo*.

3.6 Inflammatory Response of the Conductive Hydrogel in Middle Cerebral Artery Occlusion Rats

The following interference groups were constructed to investigate the anti-inflammatory activity of hydrogel systems in I/R tissues (n = 4): PBS, NSCs, GelMA/NSCs and GelMA/PEDOT: PSS100/ NSCs. Day 7 was presumed to be a critical day for stem cell transplantation (L. Huang and Zhang 2019). To analyze the microglia and astrocyte responses to the implanted materials, immunostaining was performed at the ipsilateral cerebral cortex near the injection site and peri-injection site (approximately 500 μm away from the injection site) (Feig et al., 2021). The fluorescent GFAP (astrocytes) and iba1 (microglia) staining images of the injection and peri-injection locations in the MCAO brain are presented in **Figures 7A,B**. The GelMA/ PEDOT:PSS100/NSCs group had a much lower percent area of GFAP and iba1 fluorescence (**Figures 7C,E**) than the NSCs group. The percent area of GFAP and iba1 at the peri-injection location (**Figures 7D,F**) revealed no significant differences among the four groups. These findings indicated that the inflammatory responses in cerebral I/R tissues were lower than those seen in the PBS, particularly NSCs with GelMA/PEDOT: PSS100 hydrogels.

4 DISCUSSION

A conductive hydrogel scaffold with a high water content and filled with NSCs was designed for the treatment of stroke. This study is based on the complicated electrical conduction excitability and soft mechanical properties of brain tissues. According to characterization of the conductive hydrogels, the storage modulus of the GelMA/PEDOT:PSS hydrogel was affected by the mass ratio of GelMA and PEDOT:PSS,and PSS addition improved the storage modulus of the hydrogel by 1.92–3.64 kPa. It is critical to match the elastic modulus of the hydrogel to that of the rat brain as this allows the hydrogel to endure physical pressure from the surrounding brain tissue, maintain its shape after implantation, and protest the loaded NSCs (Weickenmeier et al., 2018). Our findings suggest that in

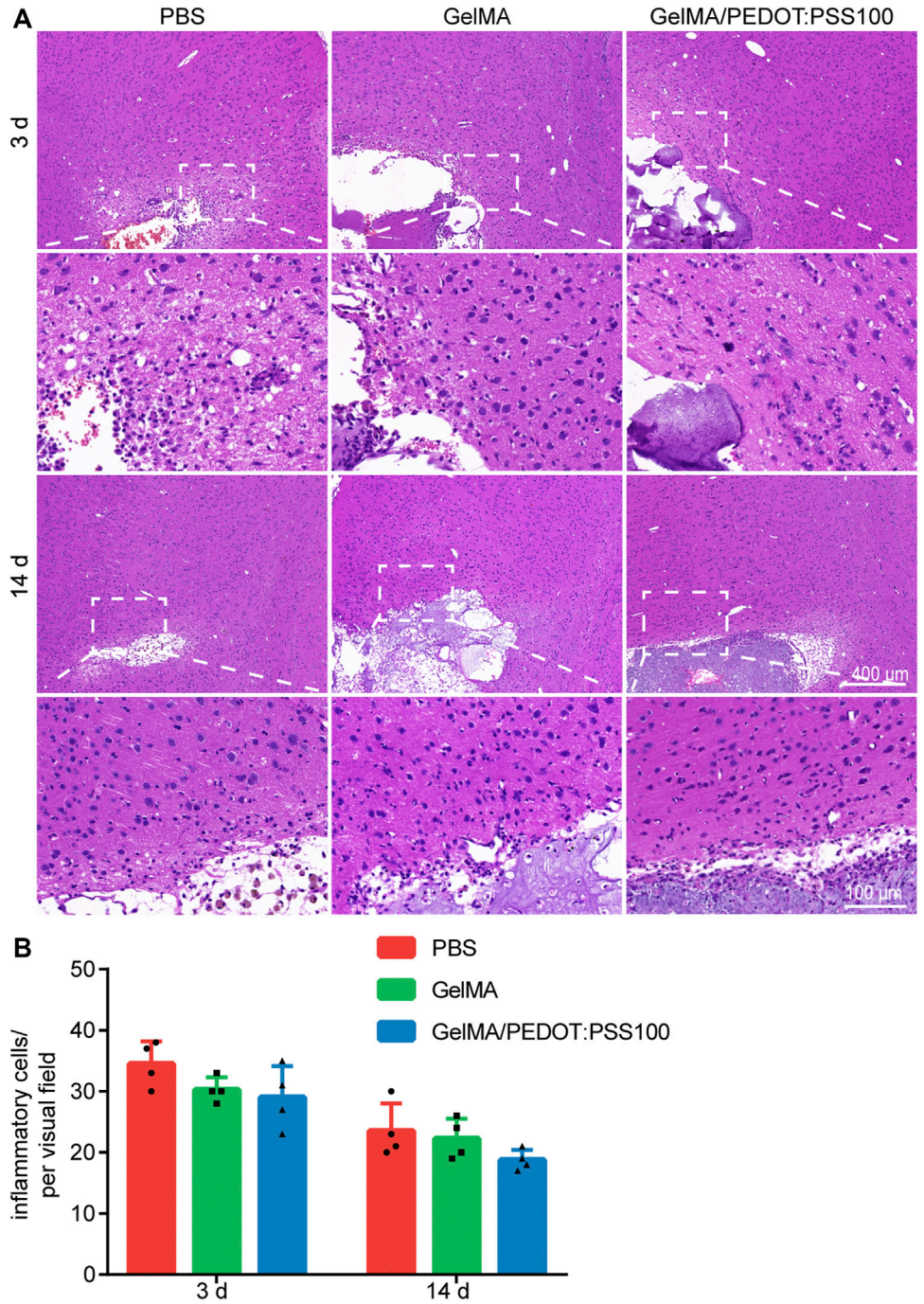

FIGURE 6 | HE staining images of different hydrogel groups 3 and 14 days after implantation. **(A)** HE staining on day 3 and 14. **(B)** Statistics of inflammatory cells. The data are expressed as mean ± SD.

the storage modulus range, GelMA/PEDOT:PSS hydrogels can provide a suitable mechanical microenvironment for nerve cells and tissues. The GelMA/PEDOT:PSS conductive hydrogel exhibits good tensile/compression mechanical capabilities, as indicated by the results of the repeated compression testing. PEDOT/PSS is a polymer that does not affect the regularity of the hydrogel molecular chain; instead, it is doped onto the hydrogel network structure as a conductive component. As a result, there will be minimal change in the tensile characteristics of the hydrogel.

An ideal material used in neural tissue engineering should have a certain electrical conductivity, allowing electrical signals to pass through the material scaffold, regulate cell activity, and stimulate nerve regeneration. According to studies, gels have a

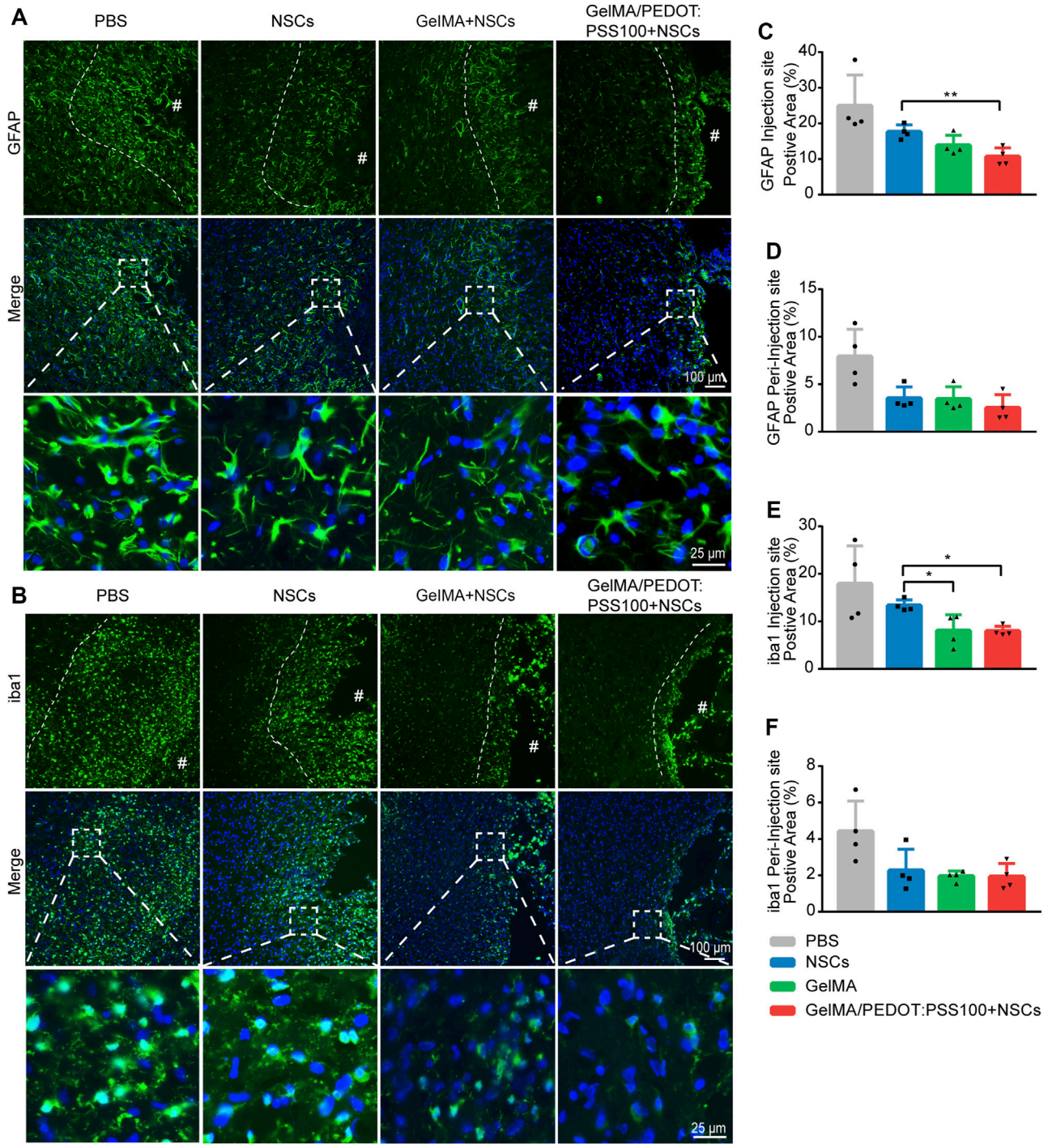

FIGURE 7 | Inflammatory response of the conductive hydrogel-loaded NSCs to cerebral I/R injury. Fluorescent images of **(A)** astrocyte (GFAP) and **(B)** microglia (iba1) staining in rat brain tissues close to the injection and peri-injection sites. The dotted lines indicate the proliferation area of astrocytes and microglia surrounding the site of injection. Quantitative analysis of GFAP positive area at the injection **(C)** and peri-injection **(D)** sites. Quantitative analysis of iba1 positive area at the injection **(E)** and peri-injection **(F)** sites. The data are expressed as mean ± SD. $^{*}p < 0.05$ and $^{**}p < 0.01$.

conductivity of approximately 10^{-7}–10^{-2} S/cm, which can be used to convey electrical signals from an organism to induce cell growth and differentiation (Zarrintaj et al., 2017). Therefore, the GelMA/PEDOT:PSS conductive hydrogel can be used in biomedical applications. The suitable conductivity criteria for conducting materials are yet to be identified. According to certain studies, only stents having an electrical conductivity of higher than 10^{-3} S/cm are viable candidates (Baniasadi et al., 2015).

Some researchers suggest that even if the conductivity is less than 10^{-3} S/cm, the hydrogel can still stimulate neuronal development, which may have no connection with the calcium channel and everything to do with its PEDOT:PSS enhances the electrostatic contact between the matrix material and the cellular anchor protein, which leads to cell differentiation (Da Silva et al., 2018). In the event of non-electrical stimulation, the regulating role of the material is stronger than the ion flow transformation. Non-electrical stimulation was used in our research to check whether the GelMA/PEDOT:PSS hydrogel, which is ideal for loading with NSCs for cerebral I/R injury, can reduce the danger of metabolic residues of conductive polymer materials *in vivo*.

Latest research on PEDOT:PSS hydrogel research was conducted using 2D culture models, which provided a better conductive contact between the cells; however, there remains a gap between the true 3D culture environments *in vivo*. Compared with the 2D culture environment, the 3D culture environment was shown to be associated with reduced cell proliferation levels (Song et al., 2019). In contrast, 3D cell encapsulation simulates the conditions that implanted cells would face *in vivo*. We were pleased to discover that at a specific concentration, PEDOT:PSS could maintain a favorable biological influence on cells and even enhance neuron metamorphosis while enhancing conductivity in a 3D culture environment. This result matched our expectations and was consistent with previous research (Fitria 2019). However, a higher concentrations of PEDOT:PSS resulted in reduced cell vitality, possibly due to the anionic PSS chain limiting cell adhesion (Spencer et al., 2018). Another cause for this could be that PEDOT:PSS is acidic, making it corrosive and poisonous. PSS components have an acidic SO3H (sulfonate acid) group on every benzene ring (Ostrakhovitch et al., 2012). Because NSCs have electrical features that distinguish them from regular adult cells, we hypothesized that they could be more sensitive to the matrix response of conductive materials. As a brain interface material, graphene has also been discovered to influence NSC differentiation by modifying the passive or active bioelectrical properties of NSCs, according to research (Huang et al., 2012). As a result, we hypothesized that NSCs cultured in 3D environments would be more electroactive in PEDOT: PSS and that NSCs would be more sensitive to external electrical ion activities. Next, we'll investigate the role of conductive materials in NSC differentiation.

We also investigated the effect of GelMA/PEDOT:PSS hydrogels loaded with NSCs on OGD/R neurons *in vitro*. It is possible because NSCs in the upper chamber shows a higher rate of development into neurons and glial cells, which secreted more brain trophic substances to impact the environment. We observed that neurospheres cultured in GelMA/PEDOT: PSS100 hydrogels could raise trophic factor transcription levels, possibly leading to an enhanced neuroprotective effect because conductive polymers can regulate trophic factors derived from stem cells, such as brain-derived neurotrophic factor (Oh and George, 2019) (**Supplementary Figure S2**).

GelMA/PEDOT:PSS/NSCs have excellent compatibility with nervous tissues as observed in our *in vivo* investigation. The mechanical damage caused by needle insertion was the primary cause of the early inflammatory reaction after hydrogel injection. After the transcranial injection, all groups in this study had the same level of inflammation level, which could be due to the mechanical damage generated by the transcranial injection. After 14 days, the number of inflammatory cells gradually decreased. Inflammatory cell infiltration into the hydrogels was noticeable, indicating that the hydrogel breakdown and integration with the surrounding tissues. The GelMA/PEDOT:PSS and GelMA hydrogel groups displayed similar inflammatory responses over the 14-days observation period, albeit a longer observation period would be required to evaluate if PEDOT: PSS sediments can cause further alterations.

The damage associated molecular patterns (DAMPs) generated by cerebral I/R injury activate resident microglia and macrophages to differentiate into a pro-inflammatory M1 phenotype. This phenotype secretes tumor necrosis factor-α, interleukin-1β and reactive oxygen species (Xiong et al., 2016). These inflammatory factors can promote the body's inflammatory response, not only changing its own structure and function, but also causing damage to surrounding tissues and indirectly promoting cell apoptosis. Following cerebral I/R injury, brain tissue expressed more proteases and hyaluronidase than normal tissue (Feig et al., 2021); as a result, hydrogels may have experienced more severe disintegration of the inflammatory response than in healthy brain tissue samples. The buildup of conductive material may result in a more severe inflammatory reaction. In contrast to the other studies (Köhler et al., 2015), we discovered that implanted NSCs loaded with GelMA/PTDOT:PSS conductive hydrogels might lower astrocyte and microglia positive areas near the inject site. It is possible that the conductive hydrogel stimulated NSC differentiation and increased neurotrophic factor secretion. In order to further confirm the neuroprotective effect of GelMA/PEDOT:PSS-loaded neural stem cells on damaged neurons, we used brain frozen section on day 7 for staining of neurons (**Supplementary Figure S3**). By observing the number of surviving neurons in the brain tissue around the injection site, it was confirmed that the GelMA/PEDOT:PSS hydrogel had a synergistic protective effect on brain neurons when loaded with neural stem cells.

5 CONCLUSION

A conductive high-water-content hydrogel scaffold filled with NSCs was designed for stroke treatment in this study, based on the complicated electrical conduction excitability and soft mechanical properties of brain tissues. *In vitro* and *in vivo* experiments proved that GelMA/PEDOT:PSS had good compatibility with neural tissue. The differentiation of neural stem cells into neurons can be promoted when 3D cultured in GelMA/PEDOT:PSS hydrogel. This conductive hydrogel loaded with NSCs could not only inhibit the apoptosis of OGD/R damaged neurons, but also improve anti-inflammatory effects of NSCs on cerebral I/R-injured tissues. Therefore, GelMA/ PEDOT: PSS hydrogels have the great potentials of regulating

NSC differentiation and serving as cell niches for cerebral I/R injury treatment.

DATA AVAILABILITY STATEMENT

The original contributions presented in the study are included in the article/**Supplementary Material**, further inquiries can be directed to the corresponding authors.

ETHICS STATEMENT

The animal study was reviewed and approved by The Ethics Committee of Zhujiang Hospital, Southern Medical University approved the Animal Research Program.

AUTHOR CONTRIBUTIONS

Conceptualization, GH, YC, and QZ; Methodology, YZ; Software, MZ; Validation, RZ; Formal analysis, HC; Investigation, XZ, and CL; Resources, HL; Data acculturation, YZ, and MZ; Writing, YZ; Visualization, MZ.; Supervision, QZ; Project administration, YC; Funding acquisition, GH. All authors have read the article carefully and agree to the published version of the manuscript.

FUNDING

This study was supported by the National Natural Science Foundation of China (82072528, 82002380 and 81874032) and Natural Science Foundation of Guangdong Province (2022A1515012460).

ACKNOWLEDGMENTS

We would like to gratefully acknowledge the support of the Animal Central Laboratory of Zhujiang Hospital, Southern Medical University.

SUPPLEMENTARY MATERIAL

The Supplementary Material for this article can be found online at: https://www.frontiersin.org/articles/10.3389/fmats.2022.914994/full#supplementary-material

REFERENCES

Abidian, M. R., Kim, D.-H., and Martin, D. C. (2006). Conducting-polymer Nanotubes for Controlled Drug Release. *Adv. Mat.* 18 (4), 405–409. doi:10.1002/adma.200501726

Bacigaluppi, M., Pluchino, S., Jametti, L. P., Kilic, E., Kilic, Ü., and Salani, G. (2009). Delayed Post-Ischaemic Neuroprotection Following Systemic Neural Stem Cell Transplantation Involves Multiple Mechanisms. *Brain* 132 (8), 2239–2251. doi:10.1093/brain/awp174

Balint, R., Cassidy, N. J., and Cartmell, S. H. (2014). Conductive Polymers: towards a Smart Biomaterial for Tissue Engineering. *Acta Biomater.* 10 (6), 2341–2353. doi:10.1016/j.actbio.2014.02.015

Baniasadi, H., Ramazani S.A., A., and Mashayekhan, S. (2015). Fabrication and Characterization of Conductive Chitosan/gelatin-Based Scaffolds for Nerve Tissue Engineering. *Int. J. Biol. Macromol.* 74, 360–366. doi:10.1016/j.ijbiomac.2014.12.014

Basara, G., Ozcebe, S. G., Ellis, B. W., and Zorlutuna, P. (2021). Tunable Human Myocardium Derived Decellularized Extracellular Matrix for 3d Bioprinting and Cardiac Tissue Engineering. *Gels* 7 (2), 70. doi:10.3390/gels7020070

Burns, T. C., and Quinones-Hinojosa, A. (2021). Regenerative Medicine for Neurological Diseases-Will Regenerative Neurosurgery Deliver? *BMJ* 373, n955. doi:10.1136/bmj.n955

Da Silva, A. C., Semeano, A. T. S., Dourado, A. H. B., Ulrich, H., and Cordoba De Torresi, S. I. (2018). Novel Conducting and Biodegradable Copolymers with Noncytotoxic Properties toward Embryonic Stem Cells. *ACS Omega* 3 (5), 5593–5604. doi:10.1021/acsomega.8b00510

De Feo, D., Merlini, A., Laterza, C., and Martino, G. (2012). Neural Stem Cell Transplantation in Central Nervous System Disorders: From Cell Replacement to Neuroprotection. *Current Opinion in Neurology* 25 (3), 322–333. doi:10.1097/WCO.0b013e328352ec45

Fann, D. Y.-W., Lee, S.-Y., Manzanero, S., Chunduri, P., Sobey, C. G., and Arumugam, T. V. (2013). Pathogenesis of Acute Stroke and the Role of Inflammasomes. *Ageing Res. Rev.* 12 (4), 941–966. doi:10.1016/j.arr.2013.09.004

Feig, V. R., Santhanam, S., McConnell, K. W., Liu, K., Azadian, M., Brunel, L. G., et al. (2021). Conducting Polymer-Based Granular Hydrogels for Injectable 3D Cell Scaffolds. *Adv. Mat. Technol.* 6 (6), 1–10. doi:10.1002/admt.202100162

Felling, R. J., and Song, H. (2015). Epigenetic Mechanisms of Neuroplasticity and the Implications for Stroke Recovery. *Exp. Neurol.* 268, 37–45. doi:10.1016/j.expneurol.2014.09.017

Fitria (2019). Development of 3D Printable Conductive Hydrogel with Crystallized PEDOT:PSS for Neural Tissue Engineering. *J. Chem. Inf. Model.* 53 (9), 1689–1699. doi:10.1016/j.msec.2019.02.008

Huang, L., and Zhang, L. (2019). Neural Stem Cell Therapies and Hypoxic-Ischemic Brain Injury. *Prog. Neurobiol.* 173, 1–17. doi:10.1016/j.pneurobio.2018.05.004

Huang, Y.-J., Wu, H.-C., Tai, N.-H., and Wang, T.-W. (2012). Carbon Nanotube Rope with Electrical Stimulation Promotes the Differentiation and Maturity of Neural Stem Cells. *Small* 8 (18), 2869–2877. doi:10.1002/smll.201200715

Ju, R., Wen, Y., Gou, R., Wang, Y., and Xu, Q. (2014). The Experimental Therapy on Brain Ischemia by Improvement of Local Angiogenesis with Tissue Engineering in the Mouse. *Cell Transpl.* 23 (Suppl. 1), S83–S95. doi:10.3727/096368914X684998

Köhler, P., Wolff, A., Ejserholm, F., Wallman, L., Schouenborg, J., and Linsmeier, C. E. (2015). Influence of Probe Flexibility and Gelatin Embedding on Neuronal Density and Glial Responses to Brain Implants. *PLOS ONE* 10 (3), e0119340. doi:10.1371/journal.pone.0119340

Lee, J. Y., Bashur, C. A., Goldstein, A. S., and Schmidt, C. E. (2009). Polypyrrole-coated Electrospun PLGA Nanofibers for Neural Tissue Applications. *Biomaterials* 30 (26), 4325–4335. doi:10.1016/j.biomaterials.2009.04.042

Levin, M., Pezzulo, G., and Finkelstein, J. M. (2017). Endogenous Bioelectric Signaling Networks: Exploiting Voltage Gradients for Control of Growth and Form. *Annu. Rev. Biomed. Eng.* 19, 353–387. doi:10.1146/annurev-bioeng-071114-040647

Li, C., Kuss, M., Kong, Y., Nie, F., Liu, X., Liu, B., et al. (2021). 3D Printed Hydrogels with Aligned Microchannels to Guide Neural Stem Cell Migration. *ACS Biomater. Sci. Eng.* 7 (2), 690–700. doi:10.1021/acsbiomaterials.0c01619

Li, H., Wang, Y., Sun, X., Tian, W., Xu, J., and Wang, J. (2019). Steady-state Behavior and Endothelialization of a Silk-Based Small-Caliber Scaffold *In Vivo* Transplantation. *Polymers* 11 (8), 1303. doi:10.3390/polym11081303

Lin, C., Li, N., Chang, H., Shen, Y., Li, Z., Wei, W., et al. (2020). Dual Effects of Thyroid Hormone on Neurons and Neurogenesis in Traumatic Brain Injury. *Cell Death Dis.* 11 (8), 671. doi:10.1038/s41419-020-02836-9

Liu, Q., Fan, X., Zhu, J., Xu, G., Li, Y., and Liu, X. (2014). Co-culturing Improves the OGD-Injured Neuron Repairing and NSCs Differentiation via Notch Pathway Activation. *Neurosci. Lett.* 559, 1–6. doi:10.1016/j.neulet.2013.11.027

Lu, J., Shen, X., Sun, X., Yin, H., Yang, S., Lu, C., et al. (2018). Increased Recruitment of Endogenous Stem Cells and Chondrogenic Differentiation by a Composite Scaffold Containing Bone Marrow Homing Peptide for Cartilage Regeneration. *Theranostics* 8 (18), 5039–5058. doi:10.7150/thno.26981

Naghavi, M., Abajobir, A. A., Abbafati, C., Abbas, K. M., Abd-Allah, F., Abera, S. F., et al. (2017). Global, Regional, and National Age-Sex Specific Mortality for 264 Causes of Death, 1980-2016: a Systematic Analysis for the Global Burden of Disease Study 2016. *Lancet* 390 (10100), 1151–1210. doi:10.1016/S0140-6736(17)32152-9

Ning, L., Mehta, R., Cao, C., Theus, A., Tomov, M., Zhu, N., et al. (2020). Embedded 3D Bioprinting of Gelatin Methacryloyl-Based Constructs with Highly Tunable Structural Fidelity. *ACS Appl. Mat. Interfaces* 12 (40), 44563–44577. doi:10.1021/acsami.0c15078

Oh, B., and George, P. (2019). Conductive Polymers to Modulate the Post-stroke Neural Environment. *Brain Res. Bull.* 148, 10–17. doi:10.1016/j.brainresbull.2019.02.015

Ostrakhovitch, E. A., Byers, J. C., O'Neil, K. D., and Semenikhin, O. A. (2012). Directed Differentiation of Embryonic P19 Cells and Neural Stem Cells into Neural Lineage on Conducting PEDOT-PEG and ITO Glass Substrates. *Archives Biochem. Biophysics* 528 (1), 21–31. doi:10.1016/j.abb.2012.08.006

She, Y., Shao, L., Zhang, Y., Hao, Y., Cai, Y., Cheng, Z., et al. (2019). Neuroprotective Effect of Glycosides in Buyang Huanwu Decoction on Pyroptosis Following Cerebral Ischemia-Reperfusion Injury in Rats. *J. Ethnopharmacol.* 242, 112051. doi:10.1016/j.jep.2019.112051

Song, S., Amores, D., Chen, C., McConnell, K., Oh, B., Poon, A., et al. (2019). Controlling Properties of Human Neural Progenitor Cells Using 2D and 3D Conductive Polymer Scaffolds. *Sci. Rep.* 9 (1), 19565. doi:10.1038/s41598-019-56021-w

Spencer, A. R., Primbetova, A., Koppes, A. N., Koppes, R. A., Fenniri, H., and Annabi, N. (2018). Electroconductive Gelatin Methacryloyl-PEDOT:PSS Composite Hydrogels: Design, Synthesis, and Properties. *ACS Biomater. Sci. Eng.* 4 (5), 1558–1567. doi:10.1021/acsbiomaterials.8b00135

Stonesifer, C., Corey, S., Ghanekar, S., Diamandis, Z., Acosta, S. A., and Borlongan, C. V. (2017). Stem Cell Therapy for Abrogating Stroke-Induced Neuroinflammation and Relevant Secondary Cell Death Mechanisms. *Prog. Neurobiol.* 158, 94–131. doi:10.1016/j.pneurobio.2017.07.004

Tang, Y.-H., Ma, Y.-Y., Zhang, Z.-J., Wang, Y.-T., and Yang, G.-Y. (2015). Opportunities and Challenges: Stem Cell-Based Therapy for the Treatment of Ischemic Stroke. *CNS Neurosci. Ther.* 21 (4), 337–347. doi:10.1111/cns.12386

Tuladhar, A., Obermeyer, J. M., Payne, S. L., Siu, R. C. W., Zand, S., Morshead, C. M., et al. (2020). Injectable Hydrogel Enables Local and Sustained Co-delivery to the Brain: Two Clinically Approved Biomolecules, Cyclosporine and Erythropoietin, Accelerate Functional Recovery in Rat Model of Stroke. *Biomaterials* 235, 119794. doi:10.1016/j.biomaterials.2020.119794

Tuo, Q. z., Zhang, S. t., and Lei, P. (2022). Mechanisms of Neuronal Cell Death in Ischemic Stroke and Their Therapeutic Implications. *Med. Res. Rev.* 42 (1), 259–305. doi:10.1002/med.21817

Wang, S., Guan, S., Li, W., Ge, D., Xu, J., Sun, C., et al. (2018). 3D Culture of Neural Stem Cells within Conductive PEDOT Layer-Assembled Chitosan/gelatin Scaffolds for Neural Tissue Engineering. *Mater. Sci. Eng. C* 93, 890–901. doi:10.1016/j.msec.2018.08.054

Wang, S., Guan, S., Zhu, Z., Li, W., Liu, T., and Ma, X. (2017). Hyaluronic Acid Doped-Poly(3,4-Ethylenedioxythiophene)/chitosan/gelatin (PEDOT-HA/Cs/gel) Porous Conductive Scaffold for Nerve Regeneration. *Mater. Sci. Eng. C* 71, 308–316. doi:10.1016/j.msec.2016.10.029

Weickenmeier, J., Kurt, M., Ozkaya, E., Wintermark, M., Pauly, K. B., and Kuhl, E. (2018). Magnetic Resonance Elastography of the Brain: A Comparison between Pigs and Humans. *J. Mech. Behav. Biomed. Mater.* 77, 702–710. doi:10.1016/j.jmbbm.2017.08.029

Woerly, S. (1993). Hydrogels for Neural Tissue Reconstruction and Transplantation. *Biomaterials* 14 (14), 1056–1058. doi:10.1016/0142-9612(93)90205-g

Xiong, X. Y., Liu, L. Y., and Yang, Q. W. (2016). Functions and Mechanisms of Microglia/Macrophages in Neuroinflammation and Neurogenesis After Stroke. *Progress in Neurobiology* 142, 23–44. doi:10.1016/j.pneurobio.2016.05.001

Yang, J., and Martin, D. C. (2004). Microporous Conducting Polymers on Neural Microelectrode Arrays. *Sensors Actuators A Phys.* 113 (2), 204–211. doi:10.1016/j.sna.2004.02.029

Ying, G., Jiang, N., Parra, C., Tang, G., Zhang, J., Wang, H., et al. (2020). Bioprinted Injectable Hierarchically Porous Gelatin Methacryloyl Hydrogel Constructs with Shape-Memory Properties. *Adv. Funct. Mat.* 30 (46), 1–13. doi:10.1002/adfm.202003740

Yuan, Z., Yuan, X., Zhao, Y., Cai, Q., Wang, Y., Luo, R., et al. (2021). Injectable GelMA Cryogel Microspheres for Modularized Cell Delivery and Potential Vascularized Bone Regeneration. *Small* 17 (11), e2006596. doi:10.1002/smll.202006596

Zarrintaj, P., Bakhshandeh, B., Rezaeian, I., Heshmatian, B., and Ganjali, M. R. (2017). A Novel Electroactive Agarose-Aniline Pentamer Platform as a Potential Candidate for Neural Tissue Engineering. *Sci. Rep.* 7 (1), 17187. doi:10.1038/s41598-017-17486-9

Zhao, J., Li, Y. X., Hao, Y. J., Chen, R., Zhang, J. Z., Sun, T., et al. (2013). Effects of Oxysophoridine on Rat Hippocampal Neurons Sustained Oxygen-Glucose Deprivation and Reperfusion. *CNS Neurosci. Ther.* 19 (2), 138–141. doi:10.1111/cns.12047

Zhou, G., Wang, Y., Gao, S., Fu, X., Cao, Y., Peng, Y., et al. (2021). Potential Mechanisms and Perspectives in Ischemic Stroke Treatment Using Stem Cell Therapies. *Front. Cell Dev. Biol.* 9, 646927. doi:10.3389/fcell.2021.646927

Zhou, H., Yang, H., Lu, L., Li, X., Pan, B., Fu, Z., et al. (2020). A Modified Protocol for the Isolation, Culture, and Cryopreservation of Rat Embryonic Neural Stem Cellsfied Protocol for the Isolation, Culture, and Cryopreservation of Rat Embryonic Neural Stem Cells. *Exp. Ther. Med.* 20 (6), 156. doi:10.3892/etm.2020.9285

Conflict of Interest: The authors declare that the research was conducted in the absence of any commercial or financial relationships that could be construed as a potential conflict of interest.

Publisher's Note: All claims expressed in this article are solely those of the authors and do not necessarily represent those of their affiliated organizations, or those of the publisher, the editors, and the reviewers. Any product that may be evaluated in this article, or claim that may be made by its manufacturer, is not guaranteed or endorsed by the publisher.